2368 *Biochemistry* **2010,** *49,* 2368–2379
DOI: 10.1021/bi901669q

BIOCHEMISTRY
including biophysical chemistry & molecular biology
Article

A Thiolate Anion Buried within the Hydrocarbon Ruler Perturbs PagP Lipid Acyl Chain Selection[†]

M. Adil Khan, Joel Moktar, Patrick J. Mott, and Russell E. Bishop*

Department of Biochemistry and Biomedical Sciences and Michael G. DeGroote Institute for Infectious Disease Research, McMaster University, Hamilton, Ontario, Canada L8N 3Z5

Received September 24, 2009; Revised Manuscript Received February 20, 2010

ABSTRACT: The *Escherichia coli* outer membrane phospholipid:lipid A palmitoyltransferase PagP exhibits remarkable selectivity because its binding pocket for lipid acyl chains excludes those differing in length from palmitate by a solitary methylene unit. This narrow detergent-binding hydrophobic pocket buried within the eight-strand antiparallel β-barrel is known as the hydrocarbon ruler. Gly88 lines the acyl chain binding pocket floor, and its substitution can raise the floor to correspondingly shorten the selected acyl chain. An aromatic exciton interaction between Tyr26 and Trp66 provides an intrinsic spectroscopic probe located immediately adjacent to Gly88. The Gly88Cys PagP enzyme was engineered to function as a dedicated myristoyltransferase, but the mutant enzyme instead selected both myristoyl and pentadecanoyl groups, was devoid of the exciton, and displayed a 21 °C reduction in thermal stability. We now demonstrate that the structural perturbation results from a buried thiolate anion attributed to suppression of the Cys sulfhydryl group pK_a from 9.4 in aqueous solvent to 7.5 in the hydrocarbon ruler microenvironment. The Cys thiol is sandwiched at the interface between a nonpolar and a polar β-barrel interior milieu, suggesting that local electrostatics near the otherwise hydrophobic hydrocarbon ruler pocket serve to perturb the thiol pK_a. Neutralization of the Cys thiolate anion by protonation restores wild-type exciton and thermal stability signatures to Gly88Cys PagP, which then functions as a dedicated myristoyltransferase at pH 7. Gly88Cys PagP assembled in bacterial membranes recapitulates lipid A myristoylation in vivo. Hydrocarbon ruler−exciton coupling in PagP thus reveals a thiol−thiolate ionization mechanism for modulating lipid acyl chain selection.

The outer membrane acyltransferase PagP catalyzes the transfer of a palmitate chain from the *sn*-1 position of a glycerophospholipid to the free hydroxyl group of the (*R*)-3-hydroxymyristate chain at position 2 of lipid A (endotoxin) (Figure 1) (*1*−*3*). In *Escherichia coli* and related pathogenic Gram-negative bacteria, PagP combats host immune defenses by restoring the bacterial outer membrane permeability barrier (*4*−*7*) and attenuating endotoxin signaling through the host TLR4/MD2 inflammation pathway (*8*−*11*). The *pagP* gene is transcriptionally activated through the bacterial PhoP/PhoQ virulence signal transduction network in response to membrane-perturbing antimicrobial peptides (*12*), immunological agents PagP helps the bacteria to resist (*4*, *6*, *13*). PagP thus provides a target for the development of anti-infective agents, but it also provides a tool for synthesizing novel vaccine adjuvants and endotoxin antagonists (*2*).

Despite the widespread importance of integral membrane enzymes of lipid metabolism in signal transduction and membrane biogenesis processes (*14*, *15*), their molecular mechanisms for lipid substrate interrogation remain poorly understood because many such enzymes have proven to be recalcitrant toward functional detergent extraction from the membrane environment. In contrast, PagP is a heat-stable 161-amino acid β-barrel enzyme, which intrinsically lacks Cys residues, and can reversibly unfold and refold in a defined detergent micellar enzymatic assay system (*16*). The structure of *E. coli* PagP has been determined both by solution nuclear magnetic resonance spectroscopy and by X-ray crystallography to reveal an eight-strand antiparallel β-barrel preceded by an N-terminal amphipathic α-helix (*17*, *18*). Like other β-barrel membrane proteins, the center of the PagP β-barrel is relatively rigid with more flexible external loops where the active site residues are localized. PagP alternates between two dynamically distinct states likely representing dormant and active conformations in the outer membrane environment (*19*−*21*). PagP activity is triggered by perturbations to outer membrane lipid asymmetry that allow the phospholipid and lipid A substrates to access the active site from the external leaflet by a lateral lipid diffusion mechanism through two gateways in the β-barrel wall known as the crenel and embrasure, respectively (*22*). X-ray studies of the inhibited PagP enzyme identified a single detergent molecule buried within the rigid β-barrel core, a site that corresponds with the palmitoyl group binding pocket known as the hydrocarbon ruler (Figure 2A) (*18*).

PagP is exquisitely selective for a 16-carbon palmitate chain because its hydrocarbon ruler excludes lipid acyl chains differing in length by a solitary methylene unit (*16*, *18*). Mutation of Gly88 lining the hydrocarbon ruler floor can modulate lipid acyl chain selection (*16*). Appropriate amino acid substitutions shorten the selected acyl chain by a degree predictable from the expected rise in the hydrocarbon ruler floor. The architecture of the acyl chain

[†]This work was supported by CIHR Operating Grant MOP-84329 awarded to R.E.B.

*To whom correspondence should be addressed: Department of Biochemistry and Biomedical Sciences, McMaster University, Health Sciences Centre 4H19, 1200 Main St. W., Hamilton, ON, Canada L8N 3Z5. Telephone: (905) 525-9140, ext. 28810. Fax: (905) 522-9033. E-mail: bishopr@mcmaster.ca.

 Published on Web 02/22/2010

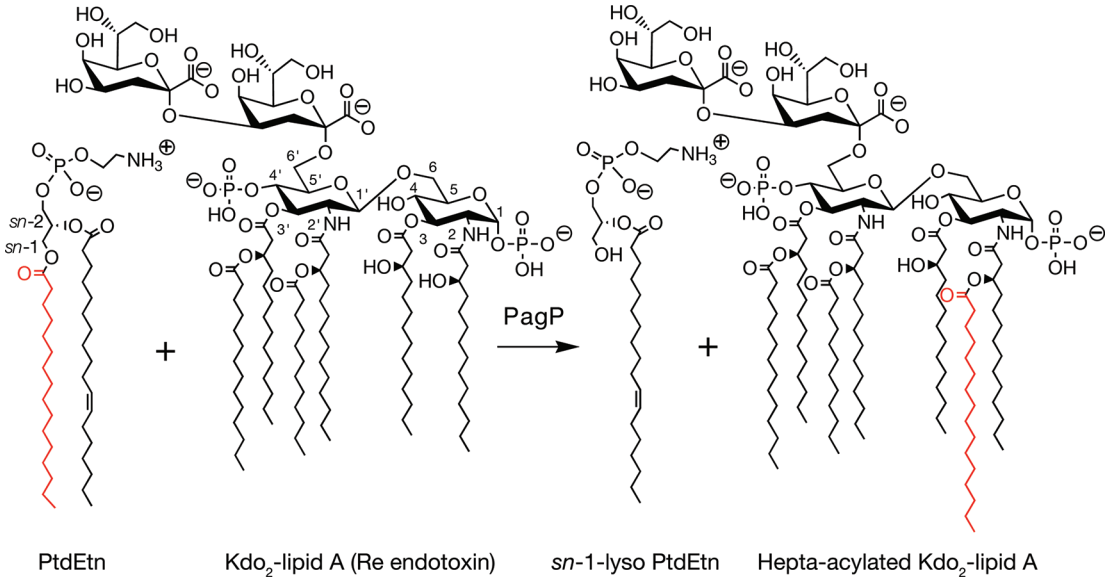

FIGURE 1: Reaction catalyzed by the phospholipid::lipid A palmitoyltransferase PagP. *E. coli* PagP transfers a palmitoyl group from the *sn*-1 position of a phospholipid, such as phosphatidylethanolamine (PtdEtn), to the free hydroxyl group of the N-linked (*R*)-3-hydroxymyristate chain on the proximal glucosamine unit of lipid A. One of the simplest lipid A acceptors for PagP in the outer membrane is known as Kdo_2-lipid A or Re endotoxin.

binding pocket can be monitored by a spectroscopic signature in circular dichroism (CD)[1] known as an aromatic exciton couplet (*16*, *23*). The exciton is a consequence of excited state delocalization between Tyr26 and Trp66 aromatic $\pi \rightarrow \pi^*$ transitions, which occurs when these residues adopt the precise geometric arrangement found near the hydrocarbon ruler floor in folded wild-type PagP (Figure 2B). The exciton couplet manifests a positive ellipticity maximum at 232 nm together with an equivalent negative ellipticity maximum at 218 nm (Figure 2D). This nondegenerate exciton couplet is the resultant of two Cotton effects where the rotational strength (R_o) and splitting energy (Δ_{ij}) each depend on an orthogonal relationship between the interaction energy (V_{ij}) and the energy difference between the two chromophore electric dipole transition moments (δ_{ij}) (Figure 2E−G) (*24*). The 218 nm signal in the PagP far-ultraviolet (far-UV) CD spectrum is the further resultant of combining the negative exciton band with the stronger Cotton effect for the polypeptide $n \rightarrow \pi^*$ transition, which also arises at 218 nm due to the β-barrel structure (*16*). The aromatic exciton thus provides an intrinsic spectroscopic probe, which was first detected by its disappearance in response to a local structural perturbation associated with PagP hydrocarbon ruler manipulation.

In our prior investigations of PagP hydrocarbon ruler mutants in which Gly88Ala, Gly88Cys-*S*-methyl, and Gly88Met mutations were introduced, acyl chain selection was predictably shifted toward C15, C13, and C12 acyl chains, respectively, with the expected unitary methylene resolution. Furthermore, these mutants displayed the exciton and the thermal melting temperature (T_m) of 88 °C characteristic of wild-type PagP (*16*). We had anticipated the Gly88Cys mutant would behave as a dedicated myristoyltransferase, but the acyl chain resolution was compromised because it selected both C14 and C15 acyl chains. Additionally, the Gly88Cys enzyme failed to display the exciton and had its T_m decreased to 67 °C (*16*). Since Cys residues are usually accommodated easily in a membrane environment (*25*), our findings suggested the sulfhydryl group in Gly88Cys PagP might be surprisingly too polar for its surrounding hydrophobic milieu. Instead of projecting up from the hydrocarbon ruler floor, we reasoned the sulfhydryl group might be stabilized by rotating around its χ_1 dihedral angle to interact with the aromatic exciton partners (*16*). This rotation would simultaneously disrupt the geometric requirements to establish the exciton and partially lower the hydrocarbon ruler floor to explain the observed selection of both C14 and C15 acyl chains (Figure 2C).

If the Cys sulfhydryl group is too polar for the hydrocarbon ruler microenvironment, we might predict substitution of Gly88 with Ser or Thr, for the introduction of a decidedly more polar hydroxyl group (*25*), would elicit a destabilizing effect at least comparable to that observed for Gly88Cys PagP. An alternative hypothesis is that the dissociation constant for ionization of the Cys88 thiol is lowered in the hydrophobic interior of PagP, resulting in the burying of a negatively charged thiolate anion. Initially, this seemed unlikely as the pK_a for a Cys thiol generally lies well above pH 8.0 (*26*), which is the optimal pH for PagP activity and is typically used in our PagP folding procedure. We fold PagP into detergent solutions from a denatured state in guanidine hydrochloride (Gdn-HCl), where the pK_a of the Cys thiol has previously been reported to be 9.4 (*27*). We have recently substituted key Pro residues at two flanking sites in the PagP transmembrane domain with Cys to establish a lateral diffusion mechanism for gating lipids between the membrane and the hydrocarbon ruler (*22*). Cys oxidation to form disulfide bonds in this study required the membrane permeable oxidizing reagent copper phenanthroline because the hydrophobic environment appears to stabilize the thiols and thereby increases their pK_a values. Assuming that the Cys located in the floor of the hydrocarbon ruler similarly experiences a hydrophobic environment, we did not anticipate

[1]Abbreviations: CD, circular dichroism; Kdo, 3-deoxy-D-*manno*-oct-2-ulosonic acid; DDM, *n*-dodecyl β-D-maltoside; ESI-MS, electrospray ionization mass spectrometry; EDTA, ethylenediaminetetraacetic acid; Gdn-HCl, guanidine hydrochloride; LDAO, lauryldimethylamine *N*-oxide; PDB, Protein Data Bank; PtdCho, phosphatidylcholine; PtdEtn, phosphatidylethanolamine; T_m, thermal melting temperature; TLC, thin layer chromatography; far-UV, far-ultraviolet.

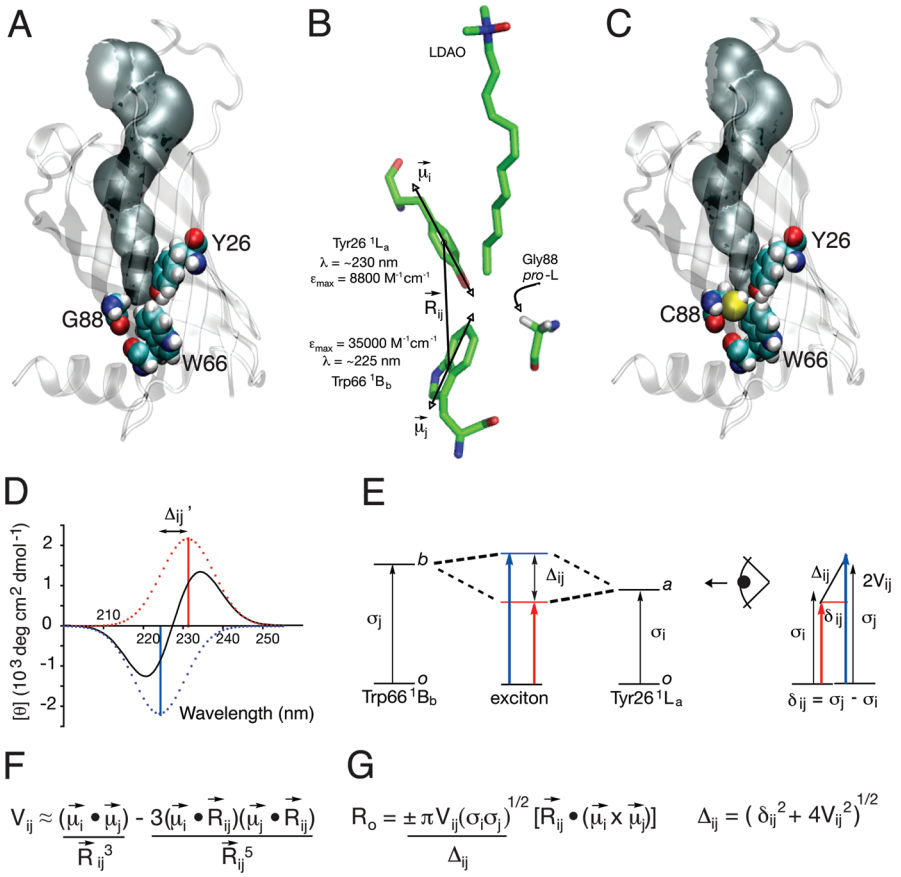

FIGURE 2: Structural relationships between the PagP hydrocarbon ruler and the aromatic exciton. (A) Structure of PagP emphasizing the hydrocarbon ruler floor residues G88, Y26, and W66. Contouring identifies the hydrocarbon ruler after the bound LDAO molecule has been removed from the crystal structure (PDB entry 1THQ). (B) The polarization axes for the interacting Tyr26 ^1L_a (μ_i) and Trp66 ^1B_b (μ_j) electric dipole transition moment vectors are shown to emphasize their relationships with the interchromophore distance vector $\mathbf{R}_{ij}$. (C) A structural perturbation hypothesis is proposed to explain the properties of Gly88Cys PagP, where a rotation of the Cys side chain perturbs the aromatic exciton partners. (D) The PagP exciton couplet (solid curve) is the resultant of two Cotton effects (red and blue dotted curves) having equal magnitude and opposite sign and separated by the exciton splitting energy Δ_{ij}, denoted as Δ_{ij}' on the wavelength scale. (E) The $\pi \rightarrow \pi^*$ transitions from ground states *o* to excited states *a* (for Tyr26 ^1L_a) or *b* (for Trp66 ^1B_b) are split by a nondegenerate exciton interaction into two new exciton states. Tyr26 and Trp66 each dominate the low-energy (red) and high-energy (blue) exciton states, respectively. The splitting energy is related to the interaction energy V_{ij} through an orthogonal relationship with the difference in the transition energies of the two chromophores ($\delta_{ij} = \sigma_j - \sigma_i$). (F) V_{ij} can be given by the point dipole approximation. (G) The theoretical rotational strengths (R_o) of nondegenerate exciton split CD Cotton effects are proportional to V_{ij}, Δ_{ij}, and a scalar triple product involving the vector connecting the centers of the two transitions and the dipole transition moments. Δ_{ij} is given by the Pythagorean theorem and reduces to $2V_{ij}$ when identical chromophores interact in the degenerate exciton condition where $\sigma_j = \sigma_i$, which in combination reduces the constant term in the equation for R_o to $\pm\pi\sigma/2$.

that the thiol pK_a would instead be suppressed. However, the pK_a for the Cys thiol in folded proteins is among the most variable of those of ionizable groups (*28*), indicative of a high sensitivity to its surrounding microenvironment. The hypothesis that a buried thiolate anion is the source of the compromised acyl chain selectivity in Gly88Cys PagP could be tested if the pH optimum for enzymatic activity is sufficiently broad across the actual Cys pK_a.

Here we report that Gly88Ser and Gly88Thr PagP enzymes display the aromatic exciton and thermal stability characteristics of wild-type PagP and function predictably as dedicated myristoyltransferases. However, folding Gly88Cys PagP from Gdn-HCl into detergent was found to lower the thiol pK_a, consistent with a model for electrostatic perturbation from a buried thiolate anion. This thiolate can be neutralized by an appropriate pH adjustment to resolve the structural perturbation and restore methylene unit resolution. Hydrocarbon ruler−exciton coupling in Gly88Cys PagP thus reveals how lipid acyl chain selection can be modulated through a thiol−thiolate ionization mechanism.

EXPERIMENTAL PROCEDURES

DNA Manipulations and Purification of Protein and Lipid A. PagP mutants were constructed with the primer sets listed in Table S1 of the Supporting Information, using the pETCrcAHΔS vector, which incorporates a C-terminal six-His tag and lacks the N-terminal signal peptide to allow for expression as insoluble aggregates in *E. coli* BL21(DE3) as described previously (*17*). Plasmids were purified using the QIAprep spin miniprep kit (Qiagen). Site-directed mutagenesis reactions were conducted using the Quickchange protocol (Stratagene). To confirm the absence of any spurious mutations in the plasmid, sequencing from the T7 primers (Table S1 of the Supporting Information) was performed.

To express the native *pagP* gene in bacterial cells under control of its endogenous promoter, the wild-type copy in plasmid pACPagP (*21*) was transferred to pBad18 (*29*) by restriction enzyme digestion with SalI and HindIII followed by ligation and transformation using standard molecular biology procedures (*30*). Designated mutations were then constructed as

described above, but with sequencing performed using the pBAD primers (Table S1 of the Supporting Information). Native PagP and its mutant derivatives were expressed in *E. coli* NR754Δ*pagP*, an *araD*$^+$ revertant of *E. coli* MC4100 (*31*, *32*), into which the Δ*pagP::kan* allele was moved from the Keio collection (*33*) by P1 transduction (*34*) followed by excision of the *kan* cartridge (*35*).

Cells were grown in LB medium at 37 °C with ampicillin at 100 μg/mL or tetracycline at 12.5 μg/mL as appropriate (*30*). PagP was purified from cytoplasmic inclusion bodies according to an established procedure (*16*). To purify radiolabeled lipid A bearing two units of 3-deoxy-D-*manno*-oct-2-ulosonic acid (Kdo_2−lipid A), we grew a 10 mL culture of *E. coli* WBB06 on [^{32}P]orthophosphate as described previously (*36*). Lipid A acylation was evaluated in vivo by [^{32}P]orthophosphate labeling with lipopolysaccharide isolation followed by mild acid hydrolysis of the ketosidic Kdo−lipid A linkage for analysis by thin layer chromatography (TLC) as described previously (*37*). Cells were treated with ethylenediaminetetraacetic acid (EDTA) to stimulate PagP activity (*21*). Nonradioactive 250 mL cultures were grown to an A_{600} of 0.8 and treated with EDTA prior to being harvested for lipid A isolation as described previously (*38*). The dried nonradioactive lipid A samples were dissolved in a 2:3:1 chloroform/methanol/water mixture and stored at −20 °C for no more than 12 h before the samples were analyzed by electrospray ionization mass spectrometry (ESI-MS) in the negative ion mode. Modeling of PagP side chain conformations at position 88 was performed as described previously (*16*).

Mass Determination and Protein Folding. Precipitated protein samples were dissolved in a 1:1 1% formic acid/acetonitrile solution just prior to ESI-MS (*16*, *39*). The sample concentration was maintained at 1 ng/μL, and the sample was injected directly onto a Waters/Micromass Q-TOF Ultima Global (a quadrupole time-of-flight) mass spectrometer. The spectra were reconstructed using MassLynx 4.0 with the MaxEnt 1 module. ESI-MS performed on PagP and its derivatives (*16*, *39*) yielded experimental protein masses accurately matching theoretical predictions (Table S1 of the Supporting Information).

After mass determination, the remainder of the precipitated protein fractions (~50 mg) were solubilized in 5 mL of 10 mM Tris-HCl (pH 8.0) and 6 M Gdn-HCl and diluted dropwise (~1 drop per 2 s) into a stirring solution of a 10-fold molar excess of 10 mM Tris-HCl (pH 8.0) and 0.5% lauryldimethylamine *N*-oxide (LDAO) (Anatrace, Maumee, OH) at room temperature and then left to stir overnight at 4 °C. The sulfhydryl group of Gly88Cys PagP was maintained in its reduced state by addition of 20 mM β-mercaptoethanol. The solution was then applied to a 4 mL Ni^{2+} ion column resin bed charged with 50 mM $NiSO_4$ and equilibrated with 10 mM Tris-HCl (pH 8.0), 0.1% LDAO, and 5 mM imidazole. The column was washed with 10 column volumes of the equilibration buffer and 10 column volumes of 10 mM Tris-HCl (pH 8.0), 0.1% LDAO, and 20 mM imidazole. The proteins were eluted with 2 mL of 10 mM Tris-HCl (pH 8.0), 0.1% LDAO, and 250 mM imidazole. The samples were then dialyzed against 10 mM Tris-HCl (pH 8.0) and 0.1% LDAO. The protein concentration was determined using the bicinchoninic acid assay kit (Pierce) (*40*) or the Edelhoch method (*41*). The folded samples were resolved by 15% sodium dodecyl sulfate−polyacrylamide gel electrophoresis with heated and unheated samples in adjacent lanes. The heated samples were boiled at 100 °C for 10 min prior to being loaded to distinguish the folded β-forms from the heat-denatured α-forms as described previously (*16*). Folded PagP proteins were stored at −20 °C. Gly88Cys PagP was also folded as described above, but including different pH values of 5.0, 6.0, 7.0, 7.2, 7.4, 7.6, 7.8, 8.0, and 9.0. Tris was used in all instances, but the pH remained stable for all samples.

Spectroscopic Analysis. Samples to be analyzed by far-UV CD were maintained at a concentration of 0.3 mg/mL in 10 mM Tris-HCl (pH 8.0) and 0.1% LDAO. A cuvette with a path length of 1 mm was used in an Aviv 215 spectrophotometer, which was linked to a Merlin Series M25 Peltier device for temperature control. For each sample, three accumulations were averaged at a data pitch of 1 nm and a scanning speed of 10 nm/min. The temperature was maintained at 25 °C, and data sets were obtained from 200 to 260 nm. Thermal denaturation profiles were obtained by measuring the loss of minimal ellipticity of the sample. The proteins were heated from 20 to 100 °C, unless indicated otherwise, at 218 nm with a temperature slope of 2 °C/min and a response time of 16 s.

A similar analysis was performed for Gly88Cys PagP folded at different pH values. In one experiment, far-UV CD and a thermal profile at 218 nm were compared for samples at pH 5.0, 6.0, 7.0, 8.0, and 9.0. In a second experiment, identical analyses were conducted for Gly88Cys folded at pH 7.0, 7.2, 7.4, 7.6, 7.8, and 8.0. In another experiment, Gly88Cys PagP folded at pH 7.8 or 7.2 was diluted in 10 mM Tris-HCl and 0.1% LDAO buffered at pH 7.2 or 7.8, respectively, before far-UV CD scans were obtained at 25 °C, after which the samples were heated to 76 °C and then cooled to 25 °C. A second far-UV CD scan was acquired at this stage. A final thermal profile was then generated after the samples had been heated to 100 °C. The Gly88Cys PagP proteins folded at pH 7.0 or 8.0 were also diluted in 10 mM Tris-HCl and 0.25% *n*-dodecyl β-D-maltoside (DDM) buffered at pH 8.0 or 7.0, respectively. Far-UV CD scans from 220 to 240 nm were conducted at 5 min intervals for 1 h. We report the data by comparing changes in the magnitude of the positive peak at 232 nm.

Acyltransferase Assays. In a 0.5 mL microcentrifuge tube, sufficient Kdo_2−lipid A (Avanti Lipids, Alabaster, AL) was added to achieve a concentration of 10 μM in a final assay volume of 25 μL. A trace amount of [^{32}P]Kdo_2−lipid A was then added to achieve a level of 200 cpm/μL. Sufficient phosphatidylcholine (PtdCho) (Avanti Lipids) with a defined acyl chain composition was added to attain a concentration of 1 mM. Diacyl PtdCho's contained identical saturated acyl chains varying in length from C10 to C17 at both the *sn*-1 and *sn*-2 positions, whereas mixed acyl chain PtdCho's contained C14 and C16 acyl chains at the *sn*-1 and *sn*-2 positions, respectively, or vice versa. These constituents were dried under a gentle N_2 stream and subsequently dissolved in 22.5 μL of a reaction cocktail containing 0.1 M Tris-HCl (pH 8.0), 10 mM EDTA, and 0.25% DDM. The reaction was initiated by addition of 2.5 μL of PagP at a sufficient concentration to achieve a linear reaction profile. All reactions were conducted at 30 °C and were stopped by directly spotting 4 μL of the reaction mixture to the origin of a Silica Gel 60 TLC plate. The TLC plate was resolved in a $CHCl_3$/pyridine/88% formic acid/H_2O mixture (50:50:16:5, v/v) within a tightly sealed glass tank. The constituents of the tank were allowed to equilibrate for a period of 3 h prior to the exposure of the TLC plate. After the plate was dried, it was exposed to a Molecular Dynamics PhosphorImager screen overnight to visualize the reaction products, which were quantified using ImageQuant. Wild-type PagP folded in 0.1% LDAO (pH 8.0) was also diluted

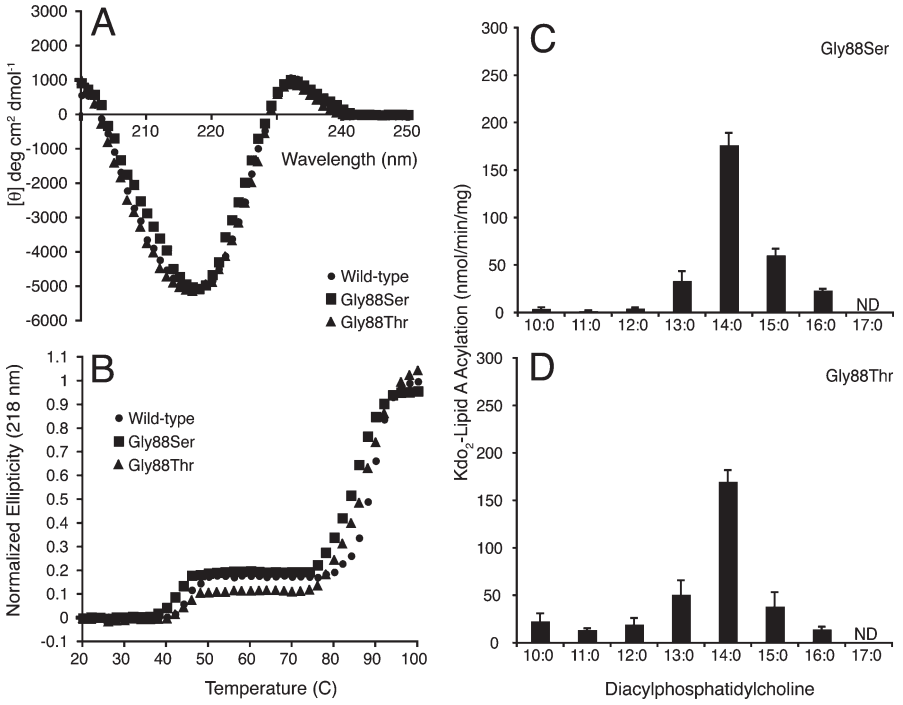

FIGURE 3: Gly88Ser and Gly88Thr PagP mutants reveal that polarity alone does not perturb acyl chain selection. (A) Far-UV CD identifies the β-barrel and exciton signatures characteristic of wild-type PagP. (B) Thermal melts at 218 nm reveal exciton loss preceding β-barrel unfolding. (C and D) Hydrocarbon ruler measurements reveal unitary acyl chain selectivity catalyzed by Gly88Ser and Gly88Thr PagP folded at pH 8. Synthetic diacyl-PtdCho's with saturated acyl chains varying in single increments from 10 to 17 carbon atoms were used as donors for the enzymatic acylation of Kdo_2−lipid A. ND, not detected.

in a reaction cocktail of 100 mM Tris-HCl, 0.25% DDM, and 10 mM EDTA at pH 5, 6, 7, 8, 9, and 10. Similarly, both wild-type and Gly88Cys PagP were folded at pH 7 and 8 and assayed at the same values to determine the effects of pH upon acyl chain selectivity.

RESULTS AND DISCUSSION

The PagP hydrocarbon ruler floor was adjusted via creation of Gly88 substitutions using site-directed mutagenesis with the primer sets shown in Table S1 of the Supporting Information and isopropyl β-D-thiogalactopyranoside-inducible PagP expression plasmid pETCrcAHΔS (*17*). The expressed proteins possess a C-terminal hexahistidine tag and lack the N-terminal signal peptide to target PagP for secretion to the outer membrane. The proteins were expressed as insoluble aggregates, which could be dissolved in Gdn-HCl, purified by Ni^{2+} ion affinity chromatography, and folded by dilution into the detergent LDAO (*16*). Mutations were confirmed both by DNA sequencing of the mutant plasmids and by ESI-MS of the purified proteins (Table S1 of the Supporting Information).

Gly88Ser and Gly88Thr PagP Mutants Are Dedicated Myristoyltransferases. To test the hypothesis that the Gly88Cys PagP structural perturbation associated with exciton loss, a 21 °C reduction in the apparent T_m, and compromised acyl chain selectivity are consequences of sulfhydryl group polarity within the hydrophobic hydrocarbon ruler environment (*16*), we additionally created the polar Gly88Ser and Gly88Thr PagP substitutions. Far-UV CD analysis of the folded mutant proteins clearly identified the positive 232 nm ellipticity known to be derived from the intact aromatic exciton (Figure 3A). Additionally, the 218 nm component of the exciton was observed by its loss at temperatures above 40 °C, consistent with the previously described thermal sensitivity of the exciton (*16*). The apparent T_m of 88 °C for wild-type PagP β-barrel unfolding was reduced by no more than 5 °C in the Gly88Ser and Gly88Thr mutants (Figure 3B).

PagP phospholipid:lipid A palmitoyltransferase activity was monitored in vitro using a defined detergent micellar enzymatic assay with TLC separation of radioactive lipid products (*16*). The inhibitory LDAO detergent used during PagP folding was exchanged by dilution into DDM to support enzymatic activity. Wild-type PagP is highly selective for a palmitoyl group at the *sn*-1 position in a glycerophospholipid, but largely unspecific for the polar headgroup (*1*). We employ the palmitoyl donor di-16:0-PtdCho and the palmitoyl acceptor [^{32}P]Kdo_2−lipid A. When challenged with a spectrum of donor acyl chain lengths, wild-type PagP is a dedicated palmitoyltransferase whereas Gly88Cys PagP utilizes both myristoyl and pentadecanoyl groups (*16*), but we found that the Gly88Ser and Gly88Thr PagP enzymes each functioned as dedicated myristoyltransferases (Figure 3C,D). These findings indicate that Cys polarity cannot explain the extinguished exciton, reduced apparent T_m, and compromised acyl chain selectivity displayed by Gly88Cys PagP (*16*) because the Ser/Thr hydroxyl group, which is more polar than the Cys sulfhydryl group (*25*), appears to be easily tolerated within the hydrocarbon ruler environment.

Exciton-Monitored Titration Reveals pK_a Suppression of the Gly88Cys PagP Thiol. To test the alternative hypothesis that the structural perturbation associated with the Gly88Cys substitution is a consequence of a buried thiolate anion, we folded Gly88Cys PagP over a range of values between pH 5 and 9 (Figure 4A,B). The absence of the exciton in Gly88Cys PagP at pH 8 was expected (*16*), but the mutant was surprisingly indistinguishable from wild-type PagP when folded at values below pH 8. The destabilization of Gly88Cys PagP at pH 8 and

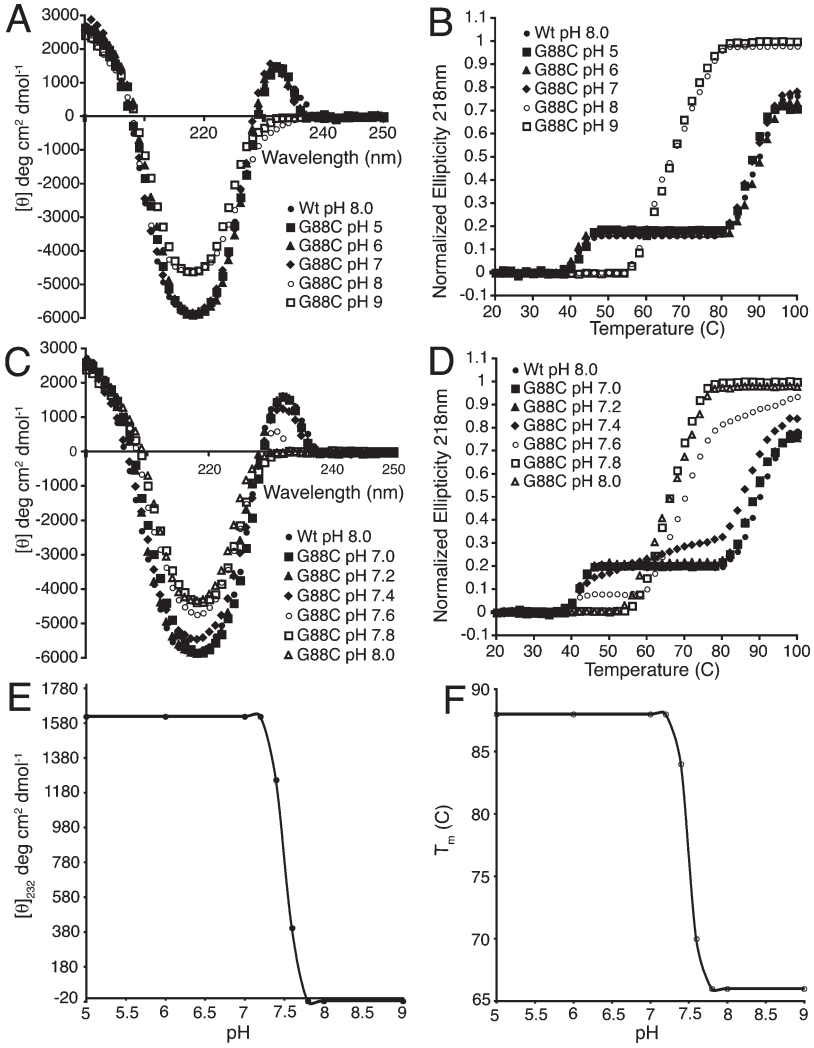

FIGURE 4: Exciton-monitored titration of the Gly88Cys PagP thiol reveals a suppressed pK_a. Far-UV CD and thermal melts for wild-type PagP folded at pH 8 and for Gly88Cys PagP over a range of pH values. (A and C) Far-UV CD wavelength scans. (B and D) Thermal melts at 218 nm. (E) pH dependence of the molar ellipticity at 232 nm. (F) pH dependence of the apparent T_m values.

above was marked by a substantial 21 °C decrease in the apparent T_m, but this decrease was undetectable at pH ≤7. In contrast, the Gly88Ser and Gly88Thr PagP mutants displayed a modest 5 °C reduction in the apparent T_m (Figure 3B), consistent with the greater polarity of the hydroxyl versus sulfhydryl group (*25*).

To identify the thiol pK_a inflection point, we repeated this experiment by folding Gly88Cys PagP at smaller increments between pH 7 and 8 (Figure 4C,D). By following the positive ellipticity at 232 nm (Figure 4E) or the apparent T_m values (Figure 4F), we could identify a sharp midpoint in both cases at pH 7.5, thus identifying the pK_a for Cys thiol ionization. These findings indicate that the Gly88Cys PagP sulfhydryl group is easily accommodated within the hydrocarbon ruler, whereas the buried thiolate anion is highly destabilizing.

Neutralizing the Thiolate Anion by Protonation in LDAO Requires PagP Thermal Unfolding. The inhibitory LDAO molecule bound in the hydrocarbon ruler presumably shields the thiol group of Gly88Cys PagP from exposure to bulk solvent. In unfolded PagP, we have previously validated the Cys thiol pK_a reported in Gdn-HCl at a value of ~9.4, which was determined by measuring the second-order rate constant for Cys thiol methylation using the alkylating agent methyl *p*-nitrobenzenesulfonate (*16*, *27*). Additionally, when PagP is folded by dilution from Gdn-HCl into LDAO, the T_m for unfolding was previously determined by differential scanning calorimetry to be 88 °C (*16*). The midpoint for β-barrel unfolding in far-UV CD thermal melts was also found to be 88 °C when the 218 nm ellipticity was monitored, but aggregation of the unfolded protein at >80 °C in this LDAO detergent system renders these precipitation curves irreversible (*16*). In contrast, the Gly88Cys PagP mutant folded at pH ≥7.8 displayed a thermal unfolding midpoint of only 67 °C (Figure 4B,D), so we reasoned that reversible folding might be observed if the system is not heated beyond 80 °C. In this case, it should be possible to expose the buried Cys thiolate to solvent at pH 7.2 and then refold the enzyme upon cooling to validate the observed pK_a of 7.5.

When Gly88Cys PagP was folded at pH 7.8 and diluted into the same LDAO detergent system at pH 7.2, the exciton remained absent from the far-UV CD spectrum, thus indicating that the buried thiolate is indeed shielded from bulk solvent (Figure 5A). When the sample was heated to 75 °C, the thermal melt confirmed the midpoint for β-barrel unfolding at 67 °C (Figure 5B). Subsequent cooling demonstrated that folding was freely reversible and established the necessary thermodynamic equilibrium to identify 67 °C as a true T_m. Interestingly, the exciton was reacquired below 50 °C and became fully evident in the wavelength scan after cooling was complete (Figure 5A,B). This observation indicates that exposure of the destabilizing thiolate anion to the

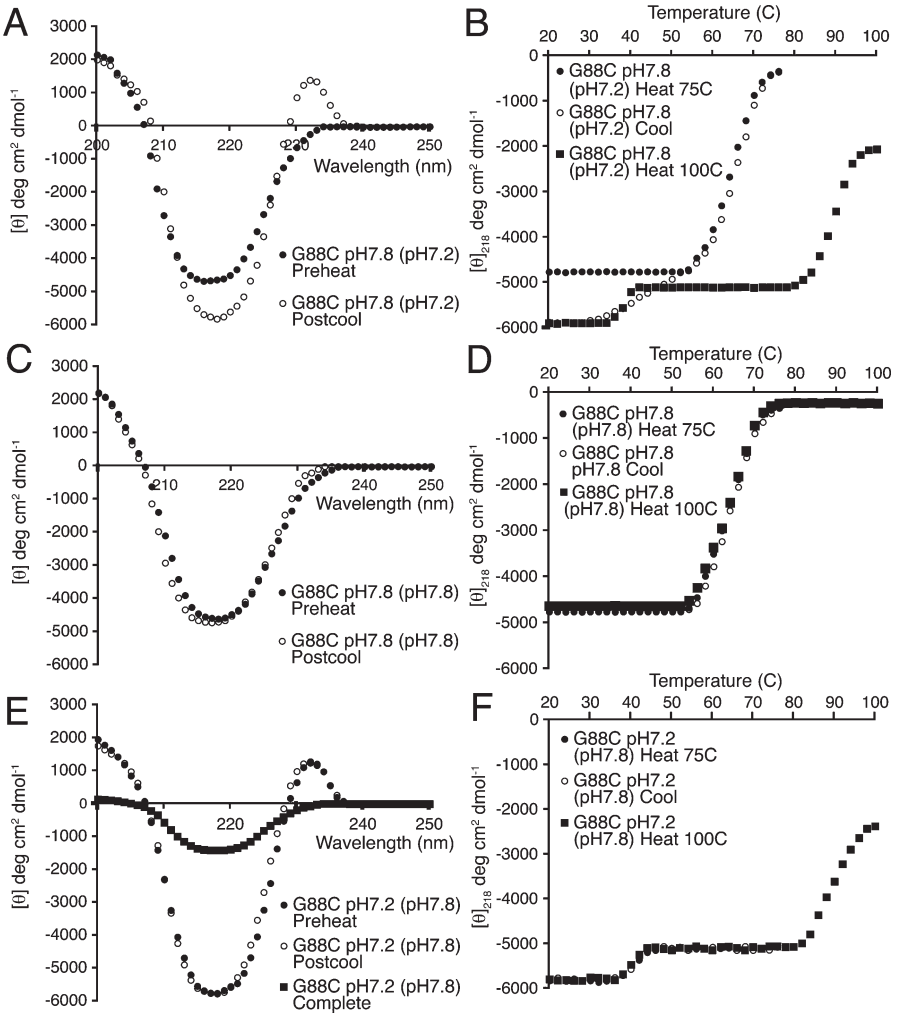

FIGURE 5: Gly88Cys PagP in LDAO must unfold to neutralize the thiolate anion. PagP folded in LDAO at pH 7.8 was diluted into LDAO at pH 7.2, heated to 75 °C, cooled, and reheated to 100 °C. A) Far-UV CD and (B) thermal melts at 218 nm reveal the acquisition of the exciton after reversible unfolding and refolding. PagP folded in LDAO at pH 7.8 was diluted into LDAO also at pH 7.8, heated to 75 °C, cooled, and reheated to 100 °C. (C) Far-UV CD and (D) thermal melts at 218 nm reveal the absence of the exciton after reversible unfolding and refolding. PagP folded in LDAO at pH 7.2 was diluted into LDAO at pH 7.8, heated to 75 °C, cooled, and reheated to 100 °C. (E) Far-UV CD and (F) thermal melts at 218 nm reveal the retention of the exciton and the absence of thermal unfolding before the sample is heated to >80 °C.

lower external pH upon unfolding allowed for a now neutralized thiol to become buried upon refolding, thus restoring the exciton at the hydrocarbon ruler floor. Subsequent heating to 100 °C revealed the thermal unfolding profile characteristic of Gly88Cys PagP folded at pH 7.2 (Figures 4D and 5B). This result was a consequence of the pH difference created upon dilution, rather than a structural reorganization associated with PagP unfolding and refolding, because the exciton was not reacquired when the experiment was repeated by dilution at the same pH 7.8 (Figure 5C,D). The reverse experiment in which Gly88Cys PagP was folded at pH 7.2 and diluted into the same LDAO detergent system at pH 7.8 showed that the exciton remained intact even after 75 °C heating and cooling (Figure 5E,F), consistent with the 88 °C β-barrel T_m, which precludes unfolding without the consequence of aggregation. Indeed, the residual ellipticity observed after the samples had been heated to 100 °C (Figure 5E) represents intermolecular β-structure associated with PagP aggregation (*16*).

Gly88Cys PagP Folded in DDM Exposes Its Thiol/Thiolate to Bulk Solvent. We have previously established that LDAO binds to the PagP hydrocarbon ruler and thereby inhibits enzymatic activity (*18*). However, diluting the enzyme into certain detergents, which are too bulky to fit within the narrow hydrocarbon ruler pocket, can create a micellar environment capable of supporting PagP activity because such detergents do not compete with substrate binding (*20*). Since the Gly88Cys PagP sulfhydryl group is clearly shielded from bulk solvent when folded in LDAO, we reasoned that the detergent DDM, which is used routinely in our defined detergent micellar enzymatic assay for PagP (*16*), should expose the thiol to solvent without the requirement of first thermally unfolding the enzyme. Indeed, when Gly88Cys PagP folded in LDAO at pH 7.0 or pH 8.0 was diluted into DDM at pH 8.0 or pH 7.0, respectively, the positive exciton ellipticity at 232 nm could be lost or acquired over a period of ~50 min (Figure 6A), thus revealing a slow solvent exchange not apparent when the protein remained folded in LDAO (Figure 5). No ellipticity change was detected when these Gly88Cys PagP proteins were monitored at the same pH at which they were initially folded (not shown).

Neutralization of the Thiolate Anion by Protonation Restores Unitary Acyl Chain Selection. Diluting wild-type PagP into DDM over a range of pH values revealed an optimum for enzymatic activity of pH 8.0, but 80% of this maximal activity was still retained at pH 7.0 (Figure 6B). Since wild-type PagP

exhibited substantial activity at both pH 7 and 8 and Gly88Cys PagP exhibited a pK_a for its lone thiol of 7.5, we were in a position to establish if the structural perturbation associated with the buried thiolate anion is responsible for the compromised acyl chain selectivity. When samples were folded and assayed at pH 8.0, the hydrocarbon ruler measurements revealed the preferences of wild-type or Gly88Cys PagP for C16 or both C14 and C15 acyl chains, respectively (Figure 7A,B), as noted previously (*16*). However, folding and assaying the same enzymes at pH 7.0 restored methylene unit resolution to Gly88Cys PagP, which then functioned as a dedicated myristoyltransferase, despite the fact that wild-type PagP remained unaltered as a palmitoyltransferase (Figure 7C,D).

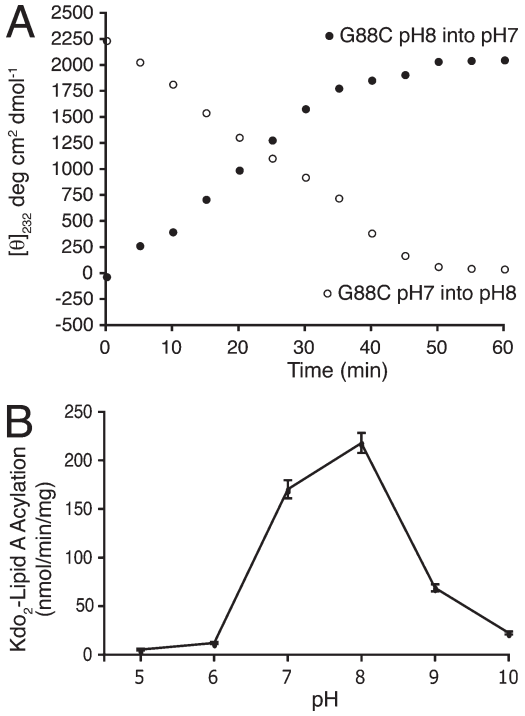

FIGURE 6: Gly88Cys PagP in DDM can expose the thiol/thiolate to solvent. (A) Gly88Cys PagP folded in LDAO at pH 8 or 7 was diluted into DDM at pH 7 or 8, respectively, and the molar ellipticity at 232 nm monitored for 60 min. (B) Wild-type PagP folded in LDAO at pH 8 was diluted into the defined detergent micellar enzymatic assay system using DDM over a range of pH values, and the acylation of Kdo_2−lipid A by dipalmitoyl-PtdCho was monitored.

Engineered PagP Myristoyltransferases Retain Regiospecificity. Wild-type PagP is highly selective for a palmitate chain, but it also selects the palmitate regiospecifically from the *sn*-1 position in the phospholipid glycerol backbone (*1*). To evaluate whether the engineered PagP myristoyltransferases display similar regiospecificity, we utilized mixed acyl chain PtdCho's having palmitate and myristate esterified to the *sn*-1 and *sn*-2 positions, respectively, or vice versa. When challenged with these mixed acyl chain PtdCho's, wild-type PagP effectively utilized only palmitate at the *sn*-1 position (Figure 8), and any residual activity from its regioisomer corresponded to the measured background utilization of myristate (Figure 7A). Exactly the opposite behavior was displayed by the engineered myristoyltransferases, thus establishing that hydrocarbon ruler modulation influenced acyl chain selectivity without affecting enzyme regiospecificity (Figure 8).

Gly88Asp, -Asn, -Glu, -Gln, -His, and -Lys PagP Mutants Retain the Exciton. If the observed structural perturbation associated with the Gly88Cys thiolate anion is a general effect of burying charge within the PagP hydrocarbon ruler, we reasoned that similar observations should be made with other charged amino acid substitutions. We engineered the acidic amino acid substitutions Gly88Asp and Gly88Glu together with their corresponding amides Gly88Asn and Gly88Gln, and the basic amino acid substitutions Gly88His and Gly88Lys (Table S1 of the Supporting Information and Figure 9). Interestingly, the exciton remained intact in all cases (Figure 9A), despite the presence

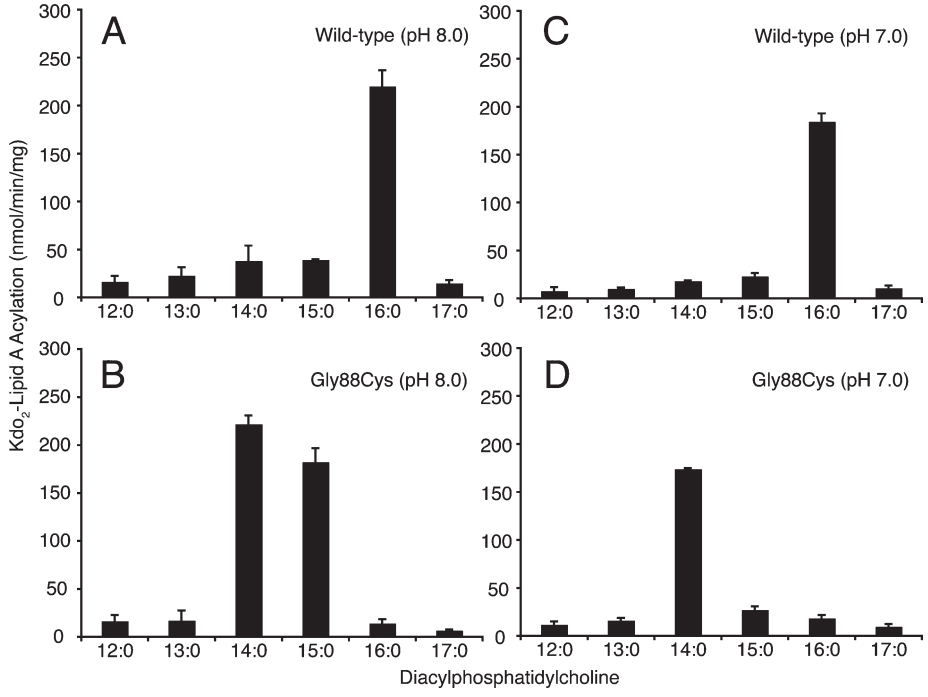

FIGURE 7: Thiol/thiolate ionization mechanism that can modulate lipid acyl chain selection. Hydrocarbon ruler experiments were performed for wild-type PagP at (A) pH 8 or (C) pH 7 and for Gly88Cys PagP at (B) pH 8 or (D) pH 7. Synthetic diacyl-PtdCho's with saturated acyl chains varying in single increments from 12 to 17 carbon atoms were used as donors for the enzymatic acylation of Kdo_2−lipid A.

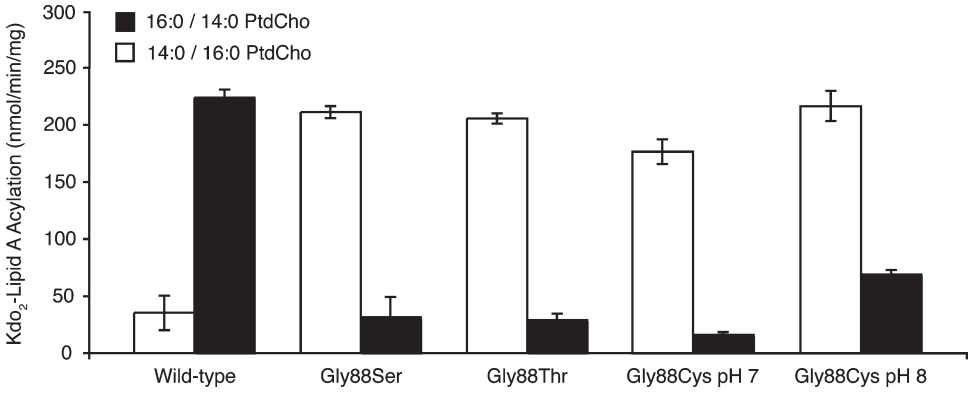

FIGURE 8: Regiospecificity of PagP palmitoyltransferase and myristoyltransferase activity. The indicated enzymes were assayed for Kdo_2−lipid A acylation using *sn*-1-palmitoyl-*sn*-2-myristoyl-PtdCho or *sn*-1-myristoyl-*sn*-2-palmitoyl-PtdCho.

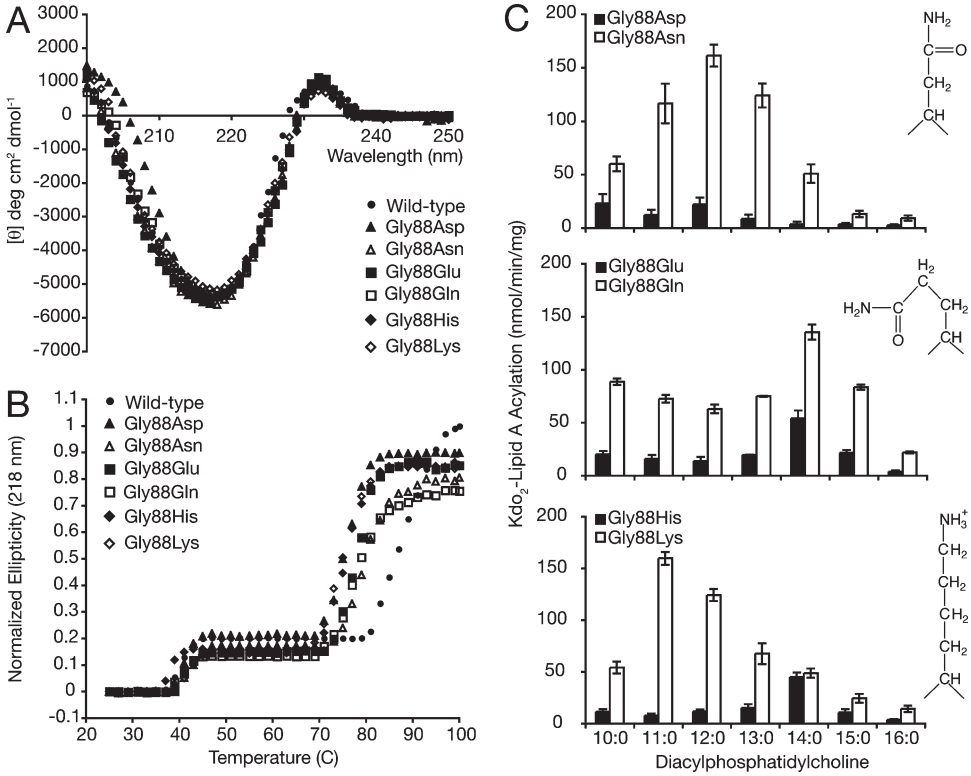

FIGURE 9: Gly88Asp, -Asn, -Glu, -Gln, -His, and -Lys PagP mutants retain the exciton. (A) Far-UV CD identifies the β-barrel and exciton signatures characteristic of wild-type PagP. (B) Thermal melts at 218 nm reveal exciton loss at 40 °C preceding β-barrel unfolding. (C) Hydrocarbon ruler measurements reveal broad acyl chain selectivity with branched or charged substitutions, but not with substitutions that are both branched and charged. Synthetic diacyl-PtdCho's with saturated acyl chains varying in single increments from 10 to 16 carbon atoms were used as donors for the enzymatic acylation of Kdo_2−lipid A. Asn/Lys and Gln amino acid side chains are shown in extended and rotated conformations, respectively.

of substantial destabilization indicated by approximate 15 and 10 °C reductions in apparent β-barrel T_m for the charged and amide substitutions, respectively (Figure 9B). Hydrocarbon ruler experiments revealed that the Gly88Asp, -Glu, and -His mutants could not support substantial enzymatic activity for any of the substrates tested, whereas the remaining substitutions could acylate Kdo_2−lipid A with maximal activities approaching 70% of that of wild-type PagP. The Gly88Asn substitution exhibited broad acyl chain selectivity centered over C12 (Figure 9C), which was approximately consistent with what might be expected if the polar branched Asn side chain projected into the hydrocarbon ruler floor in its extended conformation. However, the Gly88Gln substitution exhibited unusually broad acyl chain selectivity with a peak over C14 (Figure 9C), which could be rationalized only in terms of a Gln side chain that had rotated back upon itself. The Gly88Lys substitution shared with the Gly88Cys thiolate substitution the property of being unbranched, being charged, and accommodating acyl chains shorter than the one predicted from the length of the substitution itself (Figure 9C). Branching and charge thus appear to represent two distinct destabilizing factors when amino acid substitutions at position 88 are introduced within the PagP hydrocarbon ruler. Only groups that were both branched and charged were clearly incompatible with enzymatic activity.

In contrast to these mutants, only the Gly88Cys thiolate introduced a more pronounced 21 °C reduction in thermal stability, which was achieved distinctly at the exciton's expense (Figures 4 and 5). The exciton-proximal Cys thiolate might fit

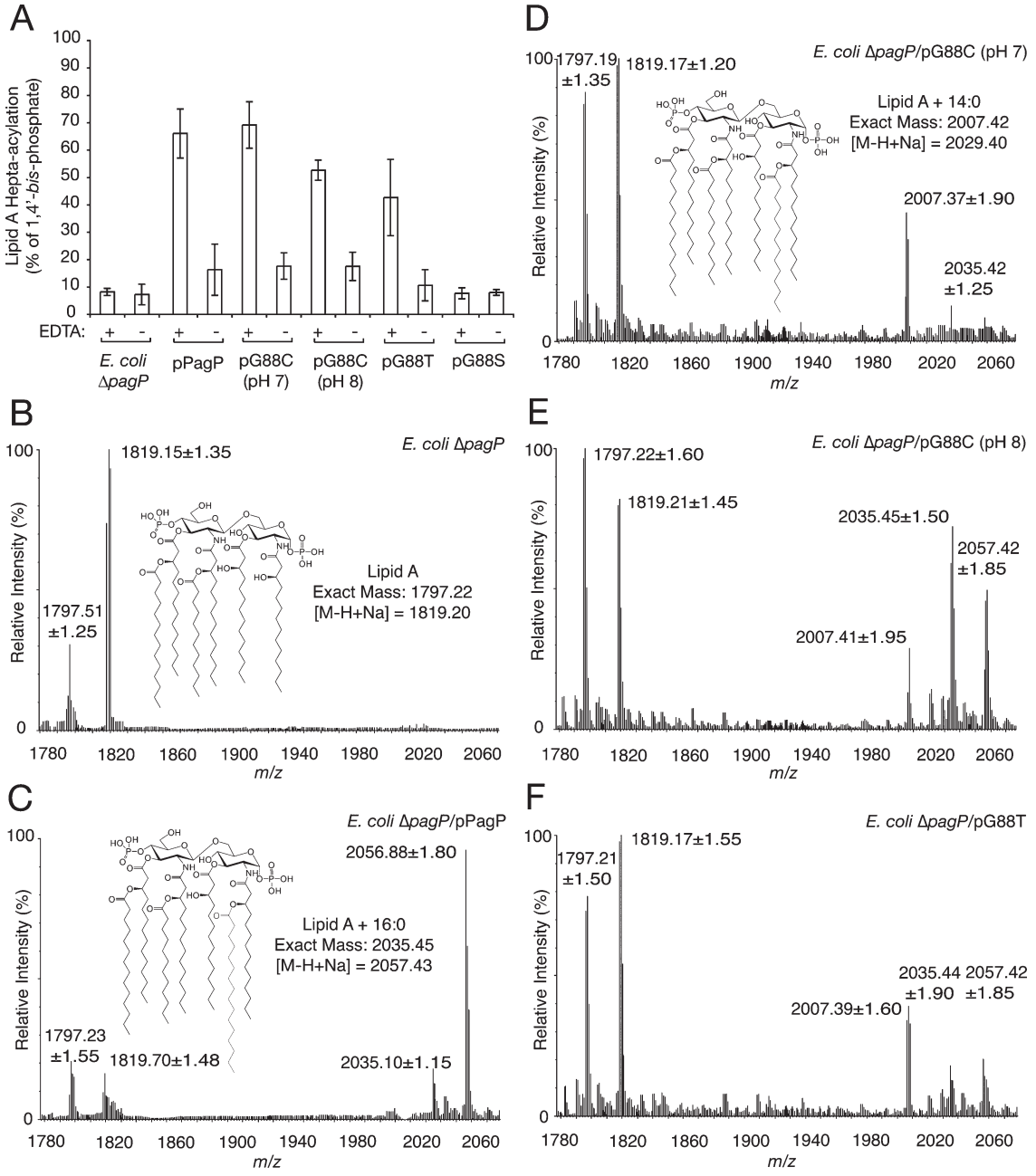

FIGURE 10: Lipid A myristoylation detected in vivo. (A) The ^{32}P-labeled lipid A 1,4′-bis-phosphate was resolved by TLC as hexa- and hepta-acylated species. The percentage of hepta-acylation in exponentially grown cultures harvested with and without EDTA treatment is shown for the *pagP* deletion strain (*E. coli* Δ*pagP*) and its transformants with plasmids pPagP, pG88C (grown at pH 7 and 8), pG88T, and pG88S. (B) ESI-MS of the lipid A 1,4′-bis-phosphate isolated from EDTA-treated *E. coli* Δ*pagP*. (C) ESI-MS of the lipid A 1,4′-bis-phosphate isolated from EDTA-treated *E. coli* Δ*pagP*/pPagP. (D) ESI-MS of the lipid A 1,4′-bis-phosphate isolated from EDTA-treated *E. coli* Δ*pagP*/pG88C (pH 7). (E) ESI-MS of the lipid A 1,4′-bis-phosphate isolated from EDTA-treated *E. coli* Δ*pagP*/pG88C (pH 8). (F) ESI-MS of the lipid A 1,4′-bis-phosphate isolated from EDTA-treated *E. coli* Δ*pagP*/pG88T.

uniquely within the hydrocarbon ruler floor as compared with the more distally positioned perturbing moieties. For example, the β-branched methyl group of Gly88Thr PagP appeared to be accommodated just as easily as that of Gly88Ser (Figure 3), thus identifying at this position an extra degree of steric freedom likely capable of accommodating a Cys thiolate side chain rotation to bring it into contact with the aromatic exciton partners as previously proposed (Figure 2C) (*16*). The apparent Gln side chain rotation occurring more distally within the PagP hydrocarbon ruler (Figure 9C) drastically compromised acyl chain selection even though the exciton remained intact. This latter point speaks to the local nature of the observed structural perturbation responsible for the loss of the exciton in Gly88Cys PagP. The distinct consequences of thiolate ionization in Gly88Cys PagP reveal not only a general effect of buried negative charge but also a role for the local context of steric and electronic constraints within the hydrocarbon ruler environment.

PagP Myristoyltransferase Mutant Activity Can Be Detected in Vivo. In exponentially growing *E. coli* cells, phospholipids are esterified with roughly 40% palmitate, 32% palmitoleate, 16% *cis*-vaccenate, 5% cyclopropane fatty acids, and another 5% attributed to myristate (*42*, *43*). Therefore, we chose to examine whether our engineered PagP myristoyltransferases could incorporate myristate into lipid A in vivo. We cloned the native *pagP* gene under control of its endogenous promoter into plasmid pBad18 (*29*) to generate pPagP. The

Gly88Cys, -Ser, and -Thr substitutions were then generated by site-directed mutagenesis to produce pG88C, pG88S, and pG88T, respectively. Each plasmid was transformed into a wild-type strain of *E. coli* K12 in which the chromosomal copy of the *pagP* gene had been deleted. Cells were grown to exponential phase and treated prior to being harvested with EDTA, which stimulates PagP activity in vivo by promoting migration of phospholipids into the external leaflet where they can access the active site by a lateral lipid diffusion mechanism (*21*, *22*). The *E. coli* outer membrane lipids are normally asymmetrically organized with lipopolysaccharide restricted to the external leaflet and phospholipids restricted to the inner leaflet, which thus maintains PagP in a latent state (*19*).

We first evaluated the incorporation of a seventh acyl chain into the hexa-acylated 1,4′-bis-phosphorylated lipid A species using ^{32}P labeling for analysis by TLC (*21*, *37*) (Figure 10A). The pG88C transformant was cultured at pH 7 and 8. Substantial production of a hepta-acylated lipid A species was detected in all PagP-expressing cells except for that of the pG88S transformant. Although the Gly88Ser mutant functions as a dedicated myristoyltransferase in vitro (Figure 3C), it appears that this mutant is not functional in vivo perhaps due to a defect in expression and/or outer membrane assembly. To evaluate the nature of the acyl chains incorporated into lipid A of EDTA-treated cells, we isolated nonradioactive lipid A for analysis by ESI-MS (*38*) (Figure 10B−F). The *E. coli* Δ*pagP* cells produced hexa-acylated lipid A, which displays a mass of 1797 Da with an associated sodium adduct with a mass of 1819 Da (Figure 10B). Transformation with pPagP was expected to result in the incorporation of a palmitate chain at position 2 (*13*, *37*), consistent with the observed mass of 2035 Da with the associated sodium adduct with a mass of 2057 Da (Figure 10C). Interestingly, the pG88C transformant grown at pH 7 incorporated a new species with a mass of 2007 Da, consistent with myristate without any associated sodium adduct (Figure 10D). Only a trace of palmitate was apparent despite its 8-fold excess over myristate in the *E. coli* phospholipid pool (*43*). When this same mutant was grown at pH 8, palmitate dominated over myristate (Figure 10E), suggesting that the buried thiolate anion associated with PagP folding at pH 8 in vitro (Figure 7B) also compromises lipid acyl chain selection in vivo. Transformation with pG88T resulted in myristate incorporation with a clear detection of palmitate (Figure 10F), consistent with the slight destabilization associated with the Gly88Thr substitution (Figure 3B) compared to Gly88Cys at pH 7 (Figure 4B). These findings indicate that trace amounts of myristate present in *E. coli* phospholipids can be selectively incorporated into lipid A by PagP myristoyltransferase mutants provided they assemble in outer membranes and are sufficiently stable to exclude the excess palmitate encountered in cellular phospholipids.

Concluding Remarks. We have demonstrated that the floor of the hydrophobic acyl chain-binding pocket in a Gly88Cys PagP mutant serves to suppress the thiol pK_a, which resulted in a local structural perturbation from a buried thiolate anion. Neutralization of the thiolate anion by protonation restored normal function and stability to the mutant enzyme. The question of why the hydrophobic pocket would suppress the thiol pK_a when the expected effect is to stabilize the protonated thiol, and thus increase the pK_a, remains. In a recent study of acetoacetate decarboxylase, the pK_a of Lys115 was perturbed downward by 4.5 log units due to the localization of the ε-amino group near the floor of a hydrophobic pocket formed by a β-barrel domain (*44*). The reduced dielectric constant of this microenvironment, which is reminiscent of the PagP hydrocarbon ruler, probably lowers the pK_a of Lys115 through a desolvation effect where the uncharged amino group is better stabilized in a hydrophobic milieu. The same reasoning applied to Cys88 in PagP predicts that the low-dielectric environment of the hydrocarbon ruler should instead increase the Cys pK_a by stabilizing the neutral thiol (*26*). A comprehensive investigation of perturbed pK_a values for catalytic groups in enzyme active sites has revealed only two mechanisms by which the pK_a of a Cys thiol can be suppressed (*26*). Interaction with the N-terminal dipole of an α-helix or formation of an ion pair between a Cys thiolate and a His imidazolium ion can suppress the thiol pK_a, but neither of these factors is apparent near the floor of the PagP hydrocarbon ruler. Nevertheless, thiols are particularly sensitive to local electrostatics, which have been previously suggested to lower the pK_a in otherwise hydrophobic environments (*45*, *46*). The thiol in Gly88Cys PagP is flanked by the low-dielectric environment of the hydrophobic acyl chain-binding pocket above and by numerous dipoles among the aromatic exciton partners and a largely polar β-barrel interior below. Therefore, details of the electrostatics located adjacent to the nonpolar milieu within the PagP interior might eventually reveal a novel mechanism for suppressing the pK_a of Cys thiols in proteins. To the best of our knowledge, the use of an identified aromatic exciton couplet as a probe to monitor the pK_a of an ionizable functional group has not been previously described in enzymology.

ACKNOWLEDGMENT

We thank Régis Pomès and Chris Neale (University of Toronto, Toronto, ON) for providing the PagP HOLE models that were first described in ref *16* and Robert Woody (Colorado State University, Fort Collins, CO) and Thomas K. Harris (University of Miami, Miami, FL) for helpful discussions. *E. coli* NR754 and plasmid pBAD18 were graciously provided by Natividad Ruiz and Thomas J. Silhavy (Princeton University, Princeton, NJ).

SUPPORTING INFORMATION AVAILABLE

Oligonucleotide primers and molecular mass determination for PagP mutants (Table S1). This material is available free of charge via the Internet at http://pubs.acs.org.

REFERENCES

1. Bishop, R. E., Gibbons, H. S., Guina, T., Trent, M. S., Miller, S. I., and Raetz, C. R. (2000) Transfer of palmitate from phospholipids to lipid A in outer membranes of Gram-negative bacteria. *EMBO J. 19*, 5071–5080.
2. Bishop, R. E. (2005) The lipid A palmitoyltransferase PagP: Molecular mechanisms and role in bacterial pathogenesis. *Mol. Microbiol. 57*, 900–912.
3. Raetz, C. R., Reynolds, C. M., Trent, M. S., and Bishop, R. E. (2007) Lipid A modification systems in Gram-negative bacteria. *Annu. Rev. Biochem. 76*, 295–329.
4. Pilione, M. R., Pishko, E. J., Preston, A., Maskell, D. J., and Harvill, E. T. (2004) *pagP* is required for resistance to antibody-mediated complement lysis during *Bordetella bronchiseptica* respiratory infection. *Infect. Immun. 72*, 2837–2842.
5. Preston, A., Maxim, E., Toland, E., Pishko, E. J., Harvill, E. T., Caroff, M., and Maskell, D. J. (2003) *Bordetella bronchiseptica* PagP is a Bvg-regulated lipid A palmitoyl transferase that is required for persistent colonization of the mouse respiratory tract. *Mol. Microbiol. 48*, 725–736.
6. Robey, M., O'Connell, W., and Cianciotto, N. P. (2001) Identification of *Legionella pneumophila rcp*, a *pagP*-like gene that confers resistance

to cationic antimicrobial peptides and promotes intracellular infection. *Infect. Immun. 69*, 4276–4286.
7. Smith, A. E., Kim, S. H., Liu, F., Jia, W., Vinogradov, E., Gyles, C. L., and Bishop, R. E. (2008) PagP activation in the outer membrane triggers R3 core oligosaccharide truncation in the cytoplasm of *Escherichia coli* O157:H7. *J. Biol. Chem. 283*, 4332–4343.
8. Kawasaki, K., Ernst, R. K., and Miller, S. I. (2004) 3-*O*-Deacylation of lipid A by PagL, a PhoP/PhoQ-regulated deacylase of *Salmonella typhimurium*, modulates signaling through toll-like receptor 4. *J. Biol. Chem. 279*, 20044–20048.
9. Miller, S. I., Ernst, R. K., and Bader, M. W. (2005) LPS, TLR4 and infectious disease diversity. *Nat. Rev. Microbiol. 3*, 36–46.
10. Muroi, M., Ohnishi, T., and Tanamoto, K. (2002) MD-2, a novel accessory molecule, is involved in species-specific actions of *Salmonella* lipid A. *Infect. Immun. 70*, 3546–3550.
11. Tanamoto, K., and Azumi, S. (2000) *Salmonella*-type heptaacylated lipid A is inactive and acts as an antagonist of lipopolysaccharide action on human line cells. *J. Immunol. 164*, 3149–3156.
12. Bader, M. W., Sanowar, S., Daley, M. E., Schneider, A. R., Cho, U., Xu, W., Klevit, R. E., Le Moual, H., and Miller, S. I. (2005) Recognition of antimicrobial peptides by a bacterial sensor kinase. *Cell 122*, 461–472.
13. Guo, L., Lim, K. B., Poduje, C. M., Daniel, M., Gunn, J. S., Hackett, M., and Miller, S. I. (1998) Lipid A acylation and bacterial resistance against vertebrate antimicrobial peptides. *Cell 95*, 189–198.
14. van Meer, G. (2005) Cellular lipidomics. *EMBO J. 24*, 3159–3165.
15. Forneris, F., and Mattevi, A. (2008) Enzymes without borders: Mobilizing substrates, delivering products. *Science 321*, 213–216.
16. Khan, M. A., Neale, C., Michaux, C., Pomes, R., Prive, G. G., Woody, R. W., and Bishop, R. E. (2007) Gauging a hydrocarbon ruler by an intrinsic exciton probe. *Biochemistry 46*, 4565–4579.
17. Hwang, P. M., Choy, W. Y., Lo, E. I., Chen, L., Forman-Kay, J. D., Raetz, C. R., Prive, G. G., Bishop, R. E., and Kay, L. E. (2002) Solution structure and dynamics of the outer membrane enzyme PagP by NMR. *Proc. Natl. Acad. Sci. U.S.A. 99*, 13560–13565.
18. Ahn, V. E., Lo, E. I., Engel, C. K., Chen, L., Hwang, P. M., Kay, L. E., Bishop, R. E., and Prive, G. G. (2004) A hydrocarbon ruler measures palmitate in the enzymatic acylation of endotoxin. *EMBO J. 23*, 2931–2941.
19. Bishop, R. E. (2008) Structural biology of membrane-intrinsic β-barrel enzymes: Sentinels of the bacterial outer membrane. *Biochim. Biophys. Acta 1778*, 1881–1896.
20. Hwang, P. M., Bishop, R. E., and Kay, L. E. (2004) The integral membrane enzyme PagP alternates between two dynamically distinct states. *Proc. Natl. Acad. Sci. U.S.A. 101*, 9618–9623.
21. Jia, W., Zoeiby, A. E., Petruzziello, T. N., Jayabalasingham, B., Seyedirashti, S., and Bishop, R. E. (2004) Lipid trafficking controls endotoxin acylation in outer membranes of *Escherichia coli*. *J. Biol. Chem. 279*, 44966–44975.
22. Khan, M. A., and Bishop, R. E. (2009) Molecular mechanism for lateral lipid diffusion between the outer membrane external leaflet and a β-barrel hydrocarbon ruler. *Biochemistry 48*, 9745–9756.
23. Grishina, I. B., and Woody, R. W. (1994) Contributions of tryptophan side chains to the circular dichroism of globular proteins: Exciton couplets and coupled oscillators. *Faraday Discuss.,* 245–262.
24. Harada, N., and Nakanishi, K. (1983) Circular dichroic spectroscopy: Exciton coupling in organic stereochemistry, University Science Books, Mill Valley, CA.
25. Bowie, J. U. (2005) Solving the membrane protein folding problem. *Nature 438*, 581–589.
26. Harris, T. K., and Turner, G. J. (2002) Structural basis of perturbed pKa values of catalytic groups in enzyme active sites. *IUBMB Life 53*, 85–98.
27. Heinrikson, R. L. (1971) The selective *S*-methylation of sulfhydryl groups in proteins and peptides with methyl-*p*-nitrobenzenesulfonate. *J. Biol. Chem. 246*, 4090–4096.
28. Pace, C. N., Grimsley, G. R., and Scholtz, J. M. (2009) Protein ionizable groups: pK values and their contribution to protein stability and solubility. *J. Biol. Chem. 284*, 13285–13289.
29. Guzman, L. M., Belin, D., Carson, M. J., and Beckwith, J. (1995) Tight regulation, modulation, and high-level expression by vectors containing the arabinose PBAD promoter. *J. Bacteriol. 177*, 4121–4130.
30. Sambrook, J., Fritsch, E. F., and Maniatis, T. (1989) Molecular cloning: A laboratory manual, 2nd ed., Cold Spring Harbor Laboratory Press, Plainview, NY.
31. Ruiz, N., Gronenberg, L. S., Kahne, D., and Silhavy, T. J. (2008) Identification of two inner-membrane proteins required for the transport of lipopolysaccharide to the outer membrane of *Escherichia coli*. *Proc. Natl. Acad. Sci. U.S.A. 105*, 5537–5542.
32. Casadaban, M. J. (1976) Transposition and fusion of the *lac* genes to selected promoters in *Escherichia coli* using bacteriophage lambda and mu. *J. Mol. Biol. 104*, 541–555.
33. Baba, T., Ara, T., Hasegawa, M., Takai, Y., Okumura, Y., Baba, M., Datsenko, K. A., Tomita, M., Wanner, B. L., and Mori, H. (2006) Construction of *Escherichia coli* K-12 in-frame, single-gene knockout mutants: The Keio collection. *Mol. Syst. Biol. 2*, 20060008.
34. Silhavy, T. J., Berman, M. L., and Enquist, L. W. (1984) Experiments with gene fusions, Cold Spring Harbor Laboratory Press, Plainview, NY.
35. Cherepanov, P. P., and Wackernagel, W. (1995) Gene disruption in *Escherichia coli*: TcR and KmR cassettes with the option of Flp-catalyzed excision of the antibiotic-resistance determinant. *Gene 158*, 9–14.
36. Kanipes, M. I., Lin, S., Cotter, R. J., and Raetz, C. R. (2001) Ca^{2+}-induced phosphoethanolamine transfer to the outer 3-deoxy-D-*manno*-octulosonic acid moiety of *Escherichia coli* lipopolysaccharide. A novel membrane enzyme dependent upon phosphatidylethanolamine. *J. Biol. Chem. 276*, 1156–1163.
37. Zhou, Z., Lin, S., Cotter, R. J., and Raetz, C. R. (1999) Lipid A modifications characteristic of *Salmonella typhimurium* are induced by NH_4VO_3 in *Escherichia coli* K12. Detection of 4-amino-4-deoxy-L-arabinose, phosphoethanolamine and palmitate. *J. Biol. Chem. 274*, 18503–18514.
38. Odegaard, T. J., Kaltashov, I. A., Cotter, R. J., Steeghs, L., van der Ley, P., Khan, S., Maskell, D. J., and Raetz, C. R. (1997) Shortened hydroxyacyl chains on lipid A of *Escherichia coli* cells expressing a foreign UDP-*N*-acetylglucosamine *O*-acyltransferase. *J. Biol. Chem. 272*, 19688–19696.
39. Whitelegge, J. P., le Coutre, J., Lee, J. C., Engel, C. K., Prive, G. G., Faull, K. F., and Kaback, H. R. (1999) Toward the bilayer proteome, electrospray ionization-mass spectrometry of large, intact transmembrane proteins. *Proc. Natl. Acad. Sci. U.S.A. 96*, 10695–10698.
40. Smith, P. K., Krohn, R. I., Hermanson, G. T., Mallia, A. K., Gartner, F. H., Provenzano, M. D., Fujimoto, E. K., Goeke, N. M., Olson, B. J., and Klenk, D. C. (1985) Measurement of protein using bicinchoninic acid. *Anal. Biochem. 150*, 76–85.
41. Edelhoch, H. (1967) Spectroscopic determination of tryptophan and tyrosine in proteins. *Biochemistry 6*, 1948–1954.
42. Oursel, D., Loutelier-Bourhis, C., Orange, N., Chevalier, S., Norris, V., and Lange, C. M. (2007) Lipid composition of membranes of *Escherichia coli* by liquid chromatography/tandem mass spectrometry using negative electrospray ionization. *Rapid Commun. Mass Spectrom. 21*, 1721–1728.
43. Cronan, J. E., Jr. (1968) Phospholipid alterations during growth of *Escherichia coli*. *J. Bacteriol. 95*, 2054–2061.
44. Ho, M. C., Menetret, J. F., Tsuruta, H., and Allen, K. N. (2009) The origin of the electrostatic perturbation in acetoacetate decarboxylase. *Nature 459*, 393–397.
45. Lo Bello, M., Parker, M. W., Desideri, A., Polticelli, F., Falconi, M., Del Boccio, G., Pennelli, A., Federici, G., and Ricci, G. (1993) Peculiar spectroscopic and kinetic properties of Cys-47 in human placental glutathione transferase. Evidence for an atypical thiolate ion pair near the active site. *J. Biol. Chem. 268*, 19033–19038.
46. Voss, J., Sun, J., Venkatesan, P., and Kaback, H. R. (1998) Sulfhydryl oxidation of mutants with cysteine in place of acidic residues in the lactose permease. *Biochemistry 37*, 8191–8196.